
Supporting information

Freestanding reduced graphene oxide-sulfur composite films for highly stable lithium-sulfur batteries

Shuwen Luo,‡[a] Minjie Yao,‡[b] Song Lei,[a] Pengze Yan,[a] Xiang Wei,[a] Xiaotong Wang,[a] Lili Liu*[a] and Zhiqiang Niu*[b]

a. Tianjin Key Laboratory for Photoelectric Materials and Devices, School of Materials Science and Engineering, Tianjin University of Technology, Tianjin, 300384, China.

E-mail: lililiuhappy@163.com.

b. Key Laboratory of Advanced Energy Materials Chemistry (Ministry of Education), College of Chemistry, Nankai University, Tianjin, 300071, P.R. China.

E-mail: zqniu@nankai.edu.cn.

1. Experimental Section

Preparation of rGO-S composite films and pure rGO films: Aqueous graphene oxide (GO) dispersions were synthesized by oxidizing graphite powder via a modified Hummers method.[1] The aqueous GO dispersion (0.4 mg mL^{-1}, 200 mL) was mixed with hydrazine monohydrate (0.08 mL) and ammonia solution (0.7 mL) in a glass vial. The vial was then heated to 90 °C for 3 hours under continuously stirring, to obtain the stable reduced graphene oxide (rGO) aqueous solution. 40 mL of as-synthesized rGO aqueous solutions were then vacuum-filtrated through an AAO template (0.2 µm pore size). The vacuum was disconnected immediately once no rGO solution was left on the filtrate cake. The rGO films together with the AAO template were then transferred to a Petri dish, and immersed into the water. After a few minutes, rGO films were automatically peeled off from the AAO template to form the solvated rGO films. The pure rGO films were obtained by freeze-drying the solvated rGO films.

The as-prepared solvated rGO films were used as precursors to fabricate freestanding rGO-S composite films. Firstly, the solvated rGO films were dipped into ethanol for 3 hours, to exchange the water remained in the films for ethanol. After several times, the solvated rGO films were then immersed into sulfur/carbon disulfide (CS_2) solution with different mass ratios (1 wt%, 2.5 wt%, 5 wt%, and 10 wt% sulfur) for 3 hours, allowing ethanol left in the film to be fully exchanged by S/CS_2 solution. Afterwards, solvated rGO films were taken out from the S/CS_2 solution, washed with ethanol for several times and subsequently immersed into water overnight to fully purge the residual CS_2 and ethanol. Finally, the solvated rGO films with infiltration of sulfur were freeze-dried to obtain binder-free freestanding rGO-S composite film. The typical area densities of resultant rGO-S films with different sulfur contents are round 1～1.5 mg cm^{-2}.

Preparation of rGO-S mixture electrode: The as-prepared rGO solution was freeze-dried to form rGO powders. Subsequently, the rGO powders (59 wt%) were mixed with sulfur powders (32 wt%) and poly(vinylidene fluoride) (PVDF) (9 wt%) in the dispersant of N-methyl-pyrrolidone (NMP) through ground in a mortar. The well-mixed slurry was cast onto an aluminum foil and then dried in a vacuum oven at 80 °C for 12 h, obtaining the rGO-S mixture cathode.

2. Sample characterization

Materials Characterization: The crystalline phases of pure sulfur powders, pure rGO film, and rGO-S composite film were identified by XRD (D-MAX/2500PC, Rigaku, Japan) with Cu Kα radiation (λ = 1.5406 Å). Morphology and structure of the rGO-S composite films were characterized by a transmission electron microscope (TEM, JEOL, JEM-2100F), and a field emission SEM (JEOL, JSM-7600F). XPS (Perkin Elmer PHI 1600 ESCA) was performed to identify the surface chemical composition and the elemental information of pure GO film and rGO-S composite film. The mass fraction of sulfur in the rGO-S composite films was tested using a TG-DSC analyzer (NETZSCH, STA 449 F3) from room temperature to 600 ℃ with a heating rate of 5 ℃ min^{-1} in N_2. The sheet resistance of the pure rGO and rGO-S composite films was measured by a semiconductor characterization system.

Electrochemical Measurements: The resultant rGO-S composite films were cut into a circle pellet with the diameter of 10 mm and directly served as the cathodes of Li-S batteries without adding carbon black or polymer binder. Both rGO-S composite films and rGO-S mixture cathodes were dried at 60 °C under vacuum for 12 h. 2032 coin-type cells using rGO-S composite (or mixture) films as the cathodes, lithium foils as the anodes, and Celgard 2320 as the separators, were assembled in an argon-filled glove box with the H_2O and O_2 contents below 1 ppm. Lithium bis(trifluoromethanesulfonyl)imide (LiTFSI, 1 M) in cosolvent of 1,3-dioxolane (DOL) and 1,2-dimethoxyethane (DME) (volume ratio 1:1) with lithium nitrate ($LiNO_3$, 0.1 M) was used as electrolyte. The cells were equilibrated for 24 h before test.

Galvanostatic charge-discharge performances were evaluated by a LAND CT2001A battery instrument at different current densities from 0.1C to 2C (1C = 1675 mA g^{-1}) within a voltage window of 1.7-2.6 V at room temperature. The CV measurements were carried out on an electrochemical workstation (CHI660E, Shanghai Chen Hua Instruments Ltd) at a scan rate of 0.1 mV s^{-1}. EIS was measured with an AC voltage amplitude of 5 mV in the frequency range of 100 mHz to 100 kHz using a Parstat 2273A potentiostat/galvanostat workstation (Princeton Applied Research & AMETEK Company).

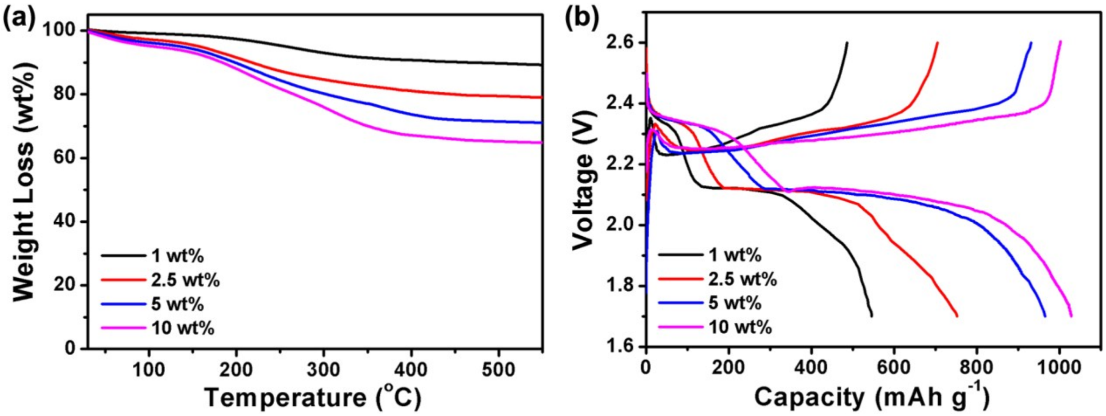

Fig. S1 (a) TGA curves and (b) First discharge/charge curves of rGO-S composite films fabricated by different mass ratios of S/CS_2 solution about 1 wt%, 2.5 wt%, 5 wt%, and 10 wt% sulfur.

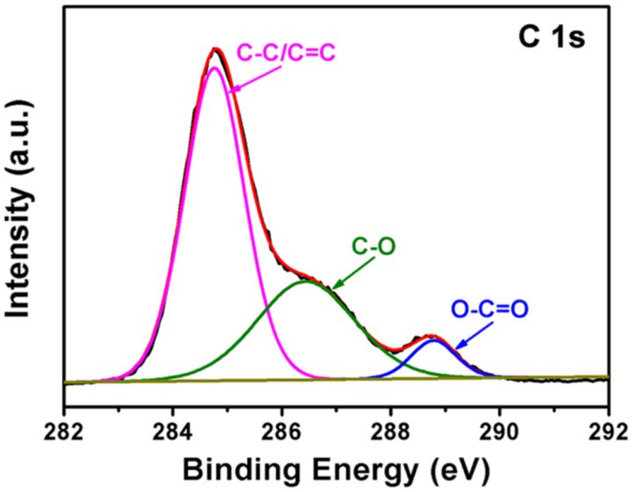

Fig. S2 High-resolution C 1s XPS spectrum of GO film.

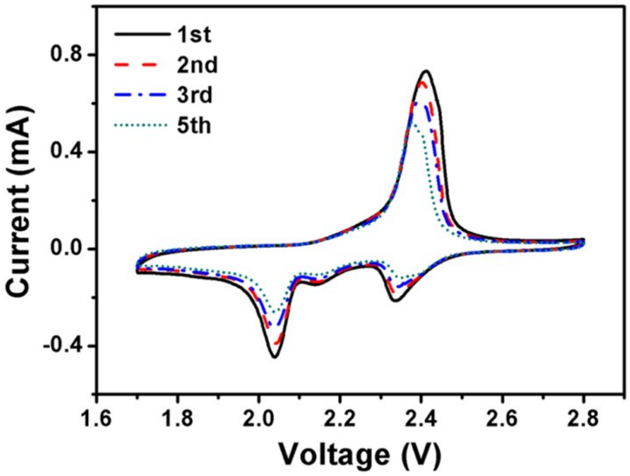

Fig. S3 CV curves of the rGO-S mixture cathode at a scan rate of 0.1 mV s^{-1} for 1st, 2nd, 3rd, and 5th cycles.

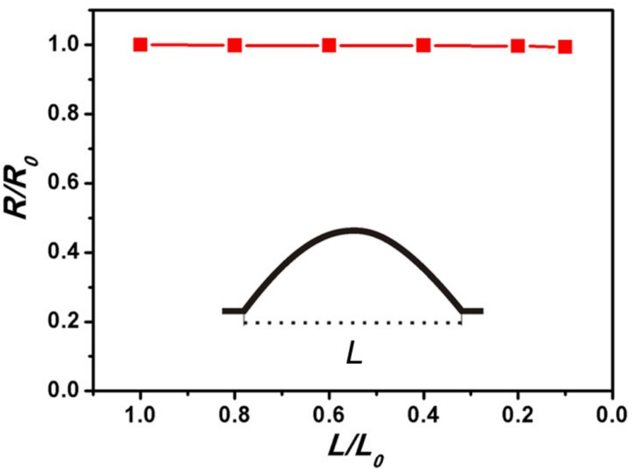

Fig. S4 The normalized sheet resistance of freestanding rGO-S composite films under different bending states. R_0 is the initial resistance and R is the resistance under different bending states; L_0 is the initial length and L is the distance between two ends of the films under different bending states.

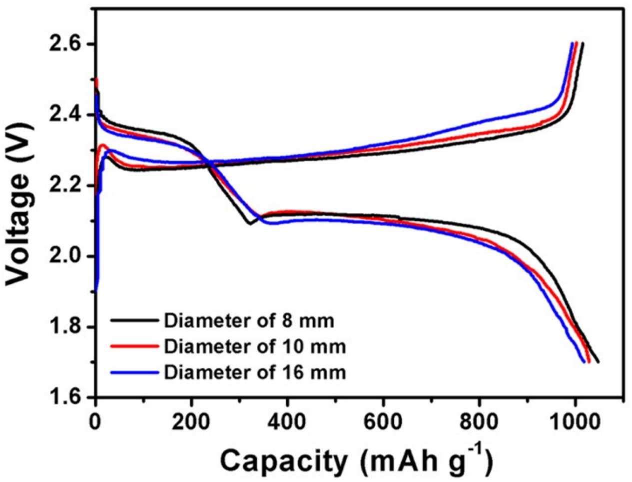

Fig. S5 First discharge/charge curves of freestanding rGO-S composite films with different sizes.

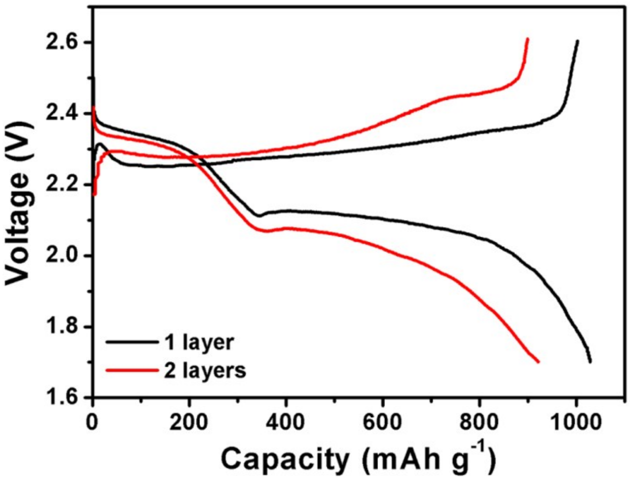

Fig. S6 First discharge/charge curves of freestanding rGO-S composite films and two-layer stacking composite films.

Table S1. The comparison of related works on graphene/S nanocomposite electrodes for Li-S batteries

	References	Methods	Additives	S content in electrode	Cycles	Capacity (mAh g^{-1})	Potential windows	Coulombic efficiency
Graphene/S hybrids	Yang et al.[2]	Reduction of GO by H_2S to form graphene/S hybrid	Super P, PVDF	32 wt%	100	0.3C 810 (initial) 576 (100 cycles)	1.5-3.0 V	94%
	Chou et al.[3]	Melt diffusion of sulfur into reduced graphene oxide	Carbon black, PVDF	42 wt%	200	0.1C 1290 (initial) 625 (200 cycles)	1.5-3.0 V	98%
	Jung et al.[4]	Melt diffusion of sulfur into graphene-SiO_2 composite	Super P, PVDF	42 wt%	40	0.1C 1189 (initial) 560 (40 cycles)	1.0-3.0 V	-
	Zhang et al.[5]	Melt diffusion of sulfur into hierarchical porous graphene	Carbon black, PVDF	46 wt%	100	1C ～824 (initial) ～450 (100 cycles)	1.5-3.0 V	–
	Zhang et al.[6]	Melt diffusion of sulfur into 3D graphene to form the S@3D-graphene composite	Carbon black, PVDF	54.75 wt%	100	0.1C 1260 (initial) ～700 (100 cycles)	1.5-3.0 V	＞96%
	Nazar et al.[7]	One-pot reaction of soluble polysulfide (Na_2S_x) with HCl to form graphene-sulfur composite	PVDF	78.3 wt%	50	0.2C 705 (initial) 550 (50 cycles)	1.5-3.0 V	93%
Freestanding graphene/S films	Hofmann et al.[8]	Infiltration of sulfur/toluene solution into the a few-layered graphene foam by drop casting	–	52 wt%	50	0.48C ～820 (initial) 518 (50 cycles)	1.5-3.0 V	99.2%
	Wang et al.[9]	Vapor treatment to introduce sulfur into a mesoporous graphene paper	–	55 wt%	50	0.1C 1393 (initial) 689 (50 cycles)	1.0-3.0 V	90%
	Yu et al.[10]	Disproportionation reaction of $Na_2S_2O_3$ with H_2SO_4 to form $PhSO_3$-RG/S composite	–	63 wt%	400	0.2C 1023 (initial) 700 (100 cycles) 460(400 cycles)	1.0-3.0 V	–

	References	Methods	Additives	S content in electrode	Cycles	Capacity (mAh g^{-1})	Potential windows	Coulombic efficiency
	Li et al.[11]	Hydrothermal reduction of GO and and sulfur mixed dispersion and freeze-drying	-	63 wt%	100	0.45C 713 (initial) 541 (100 cycles)	1.5-2.8 V	98%
	Wen et al.[12]	Vacuum infiltration of graphene sheets with sulfur nanoparticles	-	67 wt%	100	0.1C ～723 (initial) 600 (100 cycles)	1.0-3.0 V	-
	Lu et al.[13]	Vacuum filtration of G-S-CNFs coaxial nanocomposites	-	33 wt%	50	0.1C ～1047 (initial) 694 (50 cycles)	1.5-3.0 V	Around 100%
	Our work	Solution infiltration of sulfur into the solvated rGO films and freeze-drying	-	35 wt%	300	0.1C 1028 (initial) 807 (100 cycles) 721 (200 cycles) 668 (300 cycles)	1.7-2.6 V	99 %

References:

1 D. A. Dikin, S. Stankovich, E. J. Zimney, R. D. Piner, G. H. B. Dommett, G. Evmenenko, S. T. Nguyen and R. S. Ruoff, *Nature*, 2007, **448**, 457-460.

2 C. Zhang, W. Lv, W. G. Zhang, X. Y. Zheng, M. B. Wu, W. Wei, Y. Tao, Z. J. Li and Q. H. Yang, *Adv. Energy Mater.*, 2014, **4**, 1301565.

3 Y.-X. Wang, S.-L. Chou, H.-K. Liu and S.-X. Dou, *J. Power Sources*, 2013, **244**, 240-245.

4 K. H. Kim, Y.-S. Jun, J. A. Gerbec, K. A. See, G. D. Stucky and H.-T. Jung, *Carbon*, 2014, **69**, 543-551.

5 J.-Q. Huang, X.-F. Liu, Q. Zhang, C.-M. Chen, M.-Q. Zhao, S.-M. Zhang, W. Zhu, W.-Z. Qian and F. Wei, *Nano Energy*, 2013, **2**, 314-321.

6 C. Xu, Y. Wu, X. Zhao, X. Wang, G. Du, J. Zhang and J. Tu, *J. Power Sources*, 2015, **275**, 22-25.

7 S. Evers and L. F. Nazar, *Chem. Commun.*, 2012, **48**, 1233-1235.

8 K. Xi, P. R. Kidambi, R. Chen, C. Gao, X. Peng, C. Ducati, S. Hofmann and R. V. Kumar, *Nanoscale*, 2014, **6**, 5746-5753.

9 X. Huang, B. Sun, K. Li, S. Chen and G. Wang, *J. Mater. Chem. A*, 2013, **1**, 13484-13489.

10 L. Zhou, X. Lin, T. Huang and A. Yu, *J. Mater. Chem. A*, 2014, **2**, 5117-5123.

11 G. Zhou, L.-C. Yin, D.-W. Wang, L. Li, S. Pei, I. R. Gentle, F. Li and H.-M. Cheng, *ACS Nano*, 2013, **7**, 5367-5375.

12 J. Jin, Z. Wen, G. Ma, Y. Lu, Y. Cui, M. Wu, X. Liang and X. Wu, *RSC Adv.*, 2013, **3**, 2558-2560.

13 S. T. Lu, Y. W. Cheng, X. H. Wu and J. Liu, *Nano Lett.*, 2013, **13**, 2485-2489.